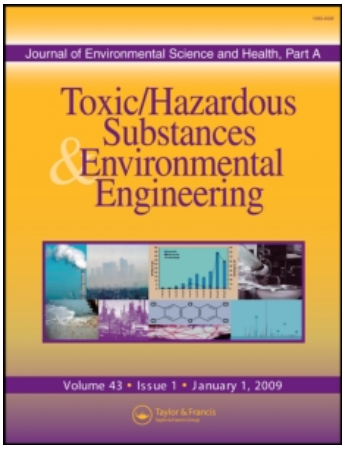

Journal of Environmental Science and Health, Part A
Publication details, including instructions for authors and subscription information:
http://www.informaworld.com/smpp/title~content=t713597268

Removal of hydroquinone from water by electrocoagulation using flow cell and optimization by response surface methodology

D. Prabhakaran [a]; C. A. Basha [b]; T. Kannadasan [c];P. Aravinthan [d]
[a] Coimbatore Institute of Technology, Coimbatore, India [b] Central Electrochemical Research Institute, Karaikudi, India [c] Centre for Research, Anna University Coimbatore, Coimbatore, India [d] Safety Health and Environment Department, Covanta Samalpatti Operating Private Limited, Parandapalli Village, India

Online publication date: 22 February 2010

To cite this Article Prabhakaran, D. , Basha, C. A. , Kannadasan, T. andAravinthan, P.(2010) 'Removal of hydroquinone from water by electrocoagulation using flow cell and optimization by response surface methodology', Journal of Environmental Science and Health, Part A, 45: 4, 400 — 412
To link to this Article: DOI: 10.1080/10934520903540174
URL: http://dx.doi.org/10.1080/10934520903540174

Journal of Environmental Science and Health Part A (2010) **45**, 400–412

ISSN: 1093-4529 (Print); 1532-4117 (Online)
DOI: 10.1080/10934520903540174

Taylor & Francis
Taylor & Francis Group

Removal of hydroquinone from water by electrocoagulation using flow cell and optimization by response surface methodology

D. PRABHAKARAN[1], C. A. BASHA[2], T. KANNADASAN[3] and P. ARAVINTHAN[4]

[1]*Coimbatore Institute of Technology, Coimbatore, India*
[2]*Central Electrochemical Research Institute, Karaikudi, India*
[3]*Centre for Research, Anna University Coimbatore, Coimbatore, India*
[4]*Safety Health and Environment Department, Covanta Samalpatti Operating Private Limited, Parandapalli Village, India*

In this study, hydroquinone was removed from water by electrocoagulation using flow electrolyzer in mono polar and bipolar configurations in a batch recirculation mode of operation. Treatment performances of such effluents have been evaluated in terms of chemical oxygen demand removal. The effect of important operating parameters such as current density, flow rate, concentration of hydroquinone and supporting electrolyte on the pollutant removal and energy consumption is critically evaluated. The experimental data were analyzed using response surface methodology (RSM). Maximum COD removal in monopolar configuration of 80.95% was noticed at condition of supporting electrolyte concentration 2.67 g L^{-1}, flow rate 27 mL min^{-1}, current density 0.7 A dm^{-2} at energy consumption of 2.36 kWh per kg of COD for the 1000 mg L^{-1} of hydroquinone concentration. In the case of bipolar configuration a maximum COD removal of 87.13 was noticed at: supporting electrolyte concentration 4 g L^{-1}, flow rate 29.15 mL min^{-1}, current density 1 Adm^{-2} at energy consumption of 8.495 kWh per kg of COD for the same hydroquinone concentration.

Keywords: Hydroquinone, electrocoagulation, mono and bipolar flow cell, response surface method.

Introduction

Rapid industrialization and urbanization resulted in the discharge of large amount of wastewater to the environment, which in turn creates more pollution. Many industries like textile, refineries, and chemical, plastic, pharmaceutical and food processing plants produce wastewaters characterized by a perceptible content of organics with strong color, high chemical oxygen demand (COD) with wide variation in pH values. Refractory organic compounds are considered as priority pollutants because of their high toxicity even at low concentrations.

Hydroquinone occurs in the environment as a result of man-made processes as well as in natural products from plants and animals. Due to its physicochemical properties, hydroquinone will be distributed mainly to the water compartment when released into the environment. It degrades both as a result of photochemical and biological processes; consequently, it does not persist in the environment. No bioaccumulation is observed. No data on hydroquinone concentrations in air, soil or water have been found. However, hydroquinone has been measured in mainstream smoke from non-filter cigarettes in amounts varying from 110 to 300 μg per cigarette, and also in side stream smoke. Hydroquinone has been found in plant-derived food products (e.g., wheat germ), in brewed coffee, and in teas prepared from the leaves of some berries where the concentration sometimes exceeds 1%.[1]

Hydroquinone (HQ) is used as raw material for herbicides, dyestuff and cosmetic product. It is highly toxic to human and aquatic organism. The major signs of poisoning include dark urine, vomiting, abdominal pain, convulsion and coma. Irritation has occurred at exposure level of 2.25 mg m^{-3} presence in water and soil has become a significant pollution problem, and effective methods for the removal or treatment need to be pursued. Wastewater treatment serves two main objectives, protecting the environment and conserving fresh water resources. Many efforts have been made for the biological treatment of wastewater rich in organic compounds. The microorganisms such as *Pseudomonas sp*,[2] *Phaneuochaere sp*[3] have been used for the degradation of organic compounds.

Address correspondence to C. Ahmed Basha, Central Electrochemical Research Institute, CSIR, Karaikudi – 630 006, Tamil Nadu, India; E-mail: basha@cecri.res.in; cab_50@rediffmail.com
Received September 10, 2009.

Biological methods have been proved to be ineffective. Effluents can be treated by biological methods, flocculation, reverse osmosis, adsorption on activated charcoal, chemical oxidation methods and advanced oxidation processes.[4] Biological methods have been proved to be ineffective.[5,6] Flocculation, reverse osmosis and adsorption methods transfer the pollutants to other media, thus causing secondary pollution.[7,8] Chemical oxidation methods are not cost effective.[9] The chemical coagulation may induce secondary pollution caused by added chemical substances. These disadvantages encouraged many studies on the use of electrocoagulation for the treatment of several industrial effluents containing refractory organic contaminants.[10]

The electrocoagulation (EC) process is based on the continuous in situ production of a coagulant in the contaminated water. It had been shown that electrocoagulation is able to eliminate a variety of pollutants from wastewaters; for example metal and arsenic,[11–13] clay minerals,[14,15] oil,[16] chemical oxygen demand,[16,17] color and organic substances.[18] Electrocoagulation is an effective technique for the treatment of effluent of various origins.[19] Compared with traditional flocculation and coagulation, EC has the advantage of removing the smallest charged particles because of the electric field sets them in motion. The characteristic of EC are simple equipment and easy operation, brief reactive retention period, decreased or negligible equipment for adding chemicals and decreased amount of sludge.[20] Therefore EC has successfully used to treat water containing food and protein wastes, synthetic detergent, effluent mine wastes and heavy metal containing solutions.[21–23] Hence, Electrocoagulation has been attracting with special interest in all applications of electrochemical treatment for the purification of wastewater.

A study has been reported where a fixed-bed reactor filled with glass sinter spools was used to investigate the dynamics and potential of methanogenic hydroquinone degradation where the concentration of hydroquinone as sole energy and carbon source in the inflowing medium varied from 550 to 2200 mg L^{-1}.[24] The bacterial community that established in the reactor after several weeks of operation was fairly stable, and consisted primarily of three bacterial species: a rod-shaped bacterium responsible for the degradation of hydroquinone to acetate and hydrogen, and two species of methanogenic bacteria, *Methanospirillum hungatei* and *Methanothix* sp.

Toxic shock due to certain chemical loads such as HQ in biological wastewater treatment systems can result in death of microorganisms and loss of floc structure. To overcome the limitations of existing approaches to toxicity monitoring, genes encoding enzymes for light production were inserted to a bacterium (Shk 1) isolated from activated sludge. The Shk 1 bioreporter indicated a toxic response to concentrations of hydroquinone (0.01 to 10,000 mg L^{-1}) by reductions in initial levels of bioluminescence on exposure to the toxicant.[25] The decrease in bioluminescence was more severe with increasing toxicant concentration. A continuous toxicity monitoring system using this bioreporter was developed for influent wastewater and tested with hydroquinone. The reporter exhibited a rapid and proportional decrease in bioluminescence in response to increasing hydroquinone concentrations.

In this study, investigations have been conducted for removal HQ by electrocoagulation using flow electrolyzer in mono and bipolar configurations in a batch recirculation mode of operation. The experiments have been carried out according to Box-Behnken design. The COD reduction and energy consumption were investigated as a function of four independent variables such as flow rate (Q), current density (CD), concentration of hydroquinone (HQ) and supporting electrolyte (SE) to explore the single and combined effect of input factors on COD reduction and optimizing the input factors using response surface methodology (RSM).

Materials and methods

Materials and analysis of chemical oxygen demand

All the chemicals used in the study were analytically pure. Laboratory grade hydroquinone was obtained from Chemport (India) Private Limited, Ambarnath (Maharashtra). Distilled water was used to prepare the desired concentration of hydroquinone (HQ) solution.

The characteristics of the wastewater such as BOD, COD, pH, solids, dissolved salts and color were estimated using the standard methods.[26] In order to determine the extent of degradation of the effluent chemical oxygen demand (COD) was measured. The COD as the name implies is the oxygen requirement of a sample for oxidation of organic and inorganic matter. COD is generally considered as the oxygen equivalent of the amount of organic matter oxidizable by potassium dichromate. The organic matter of the sample is oxidized with a known excess of potassium dichromate in a 50% sulfuric acid solution. The excess dichromate is titrated with a standard solution of ferrous ammonium sulfate solution. Experiments were repeated until the difference found less than 3%.

Response surface methodology

Response surface methodology (RSM) is a collection of statistical and mathematical methods that are useful for the modeling and analyzing engineering problems. In this technique, the main objective is to optimize the response surface that is influenced by various process parameters. Response surface methodology also quantifies the relationship between the controllable input parameters and the obtained response surfaces.[27,28] In the present study, the RSM has been used to determine the relation between the percentage of COD removal and important operating parameters such as current density (CD), flow rate(Q), concentration of hydroquinone(HQ) and supporting electrolyte(SE). Table 1

Table 1. Experimental range and levels of independent process variables for both mono polar and bipolar configuration for electrocoagulation.

			Range and levels		
Factor	*Variable*	*Unit*	*−1*	*0*	*+1*
A	HQ conc.,	mg L^{-1}	250	625	1000
B	Supporting electrolyte conc.,	g L^{-1}	1	2.5	4
C	Flow rate, Q	mL min^{-1}	25	35	45
D	Current density, CD	A dm^{-2}	0.2	0.6	1

gives the parameters and the operating ranges covered. The concentration of hydroquinone and supporting electrolyte, flow rate and current density are referred by uncoded variables as A, B, C and D, respectively.

The variables in uncoded form are converted to coded form: a, b, c and dusing the following Equation 1.

$$a = \frac{A - \left(\frac{A_{max}+A_{min}}{2}\right)}{\frac{A_{max}-A_{min}}{2}} \quad (1)$$

The Box–Behnken experimental design of RSM has been chosen to find the relationship between the response functions and variables using the statistical software package Design Expert Software-7.1.2, (Stat- Ease, Inc., Minneapolis, USA). The Box–Behnken design can be considered as a highly fractionalized three-level factorial design where the treatment combinations are the midpoints of edges of factor levels and the center point. These designs are rotatable (or nearly rotatable) and require three levels of each factor under study. Box–Behnken designs can fit full quadratic response surface models and offer advantages over other designs. The advantages of the Box–Behnken design over other response surface designs are: (a) it needs fewer experiments than central composite design and similar ones used for Doehlert designs; (b) in contrast to central composite and Doehlert designs, it has only three levels; (c) it is easier to arrange and interpret than other designs; (d) it can be expanded, contracted or even translated; and (e) it avoids combined factor extremes since midpoints of edges of factors are always used.[29]

The three level second order design demand comparatively lesser number of experimental data for precise prediction. Here, a total number of 29 experiments, including 3 centre points are carried out for 4 parameters. The interaction between the variables and the analysis of variance (ANOVA) has been studied by using RSM. The quality of the fit of this model is expressed by the coefficient of determination R^2. The fit is confirmed by means of the absolute average deviation (AAD) defined as

$$AAD = \left\{ \frac{\sum_{i=1}^{n} \left(\frac{|y_{i,exp} - y_{i,pred}|}{y_{i,exp}} \right)}{n} \right\} \times 100 \quad (2)$$

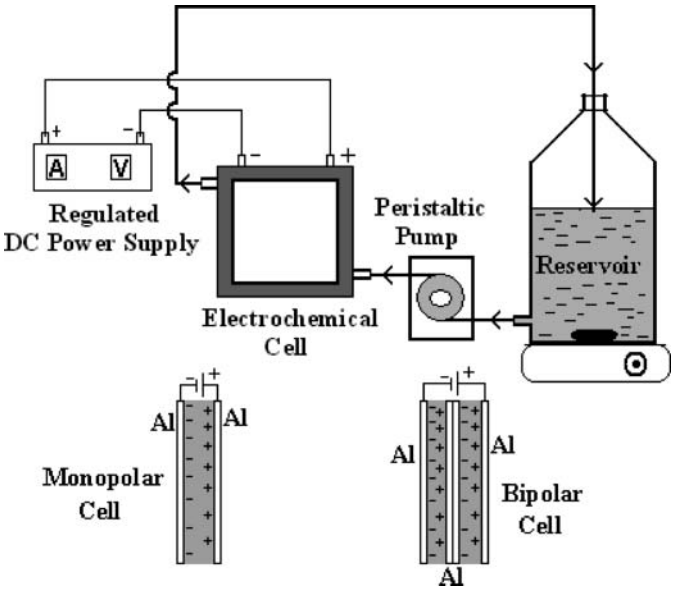

Fig. 1. Experimental setup of flow reactor.

where $y_{i,exp}$ and $y_{i,pred}$ refers the experimental and predicted responses and n refers the number of experimental runs.

Experimental setup and procedure

Monopolar configuration

The lab scale experimental setup used for the electrocoagulation studies is shown in Figure 1. The setup consists of electrochemical cell; regulated multi output DC power supply, peristaltic pump, and reservoir with the volume of 1 L. A schematic view of monopolar cell configuration is shown in Figure 2. Two aluminum electrodes were used as anode and cathode. PVC frame is used as a middle compartment. The effective surface area of anode and cathode were 7 cm × 7 cm. The electrodes were positioned vertically and parallel to each other with an inter electrode gap of 10 mm.

Electrolysis was carried out under batch recirculation mode. The effluent was taken in the reservoir, which was allowed to flow from it and was recirculated through the reactor using a peristaltic pump. The specified flow rate was adjusted. The required current was passed using regulated power supply and cell voltage was noted. The experiments where carried out six hours at different operating parameters as shown in Table 1. The One millilitre sample was drawn for every hour from the reservoir and COD was analyzed.

Bipolar configuration

The setup (see Fig. 1) consists of electrochemical cell; regulated multi output DC power supply, peristaltic pump, and

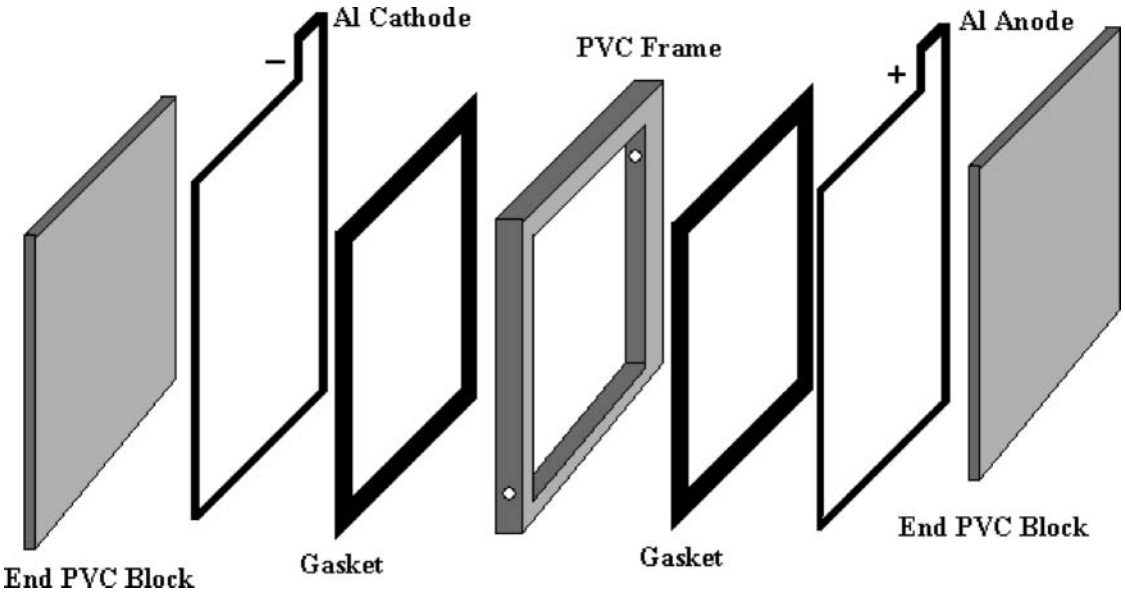

Fig. 2. Schematic view of Monopolar Electrocoagulation flow cell configuration.

reservoir. A schematic view of bipolar cell configuration is shown in Figure 3. The bipolar cell consists of 2 compartments A and B with an inlet and outlet, respectively in A and B impart. Here, 4 aluminum electrodes were used in the dimension of 9 cm × 9 cm × 0.1 cm. The working area of each of the electrode surface area is 7 cm × 7 cm. The assembly of the cell is in following manner. Two compartments are adjacent to each other; among the 4 electrodes, 2 were placed between the interface of 2 compartments, and another 2 electrodes were placed in the outer face of the compartments A & B, respectively. The volume of the electrolytic cell is 50 mL whereas the reservoir capacity is 1 L.

Electrolysis was carried out under batch continuous recirculation mode. The cyclic pathway of the effluent is as follows, the effluent is pumped by peristaltic pump into compartment A. Then it undergoes upward travels over the working area of the electrode, outlet is passed into the bottom of the compartment B, there it gets upward travels over the working area of the electrodes. After this course it returns to the reservoir tank. The required current was passed using regulated power supply and cell voltage was noted. The experiments were carried out for six hours at different operating parameters as shown in Table 1. At every hour sample was collected from the reservoir and COD was analyzed.

Reaction mechanism of electrocoagulation

Electrocoagulation is based on the in situ formation of the coagulant as the sacrificial anode corrodes due to an applied current, while the simultaneous evolution of hydrogen at the cathode allows for pollutant removal by flotation. This technique combines three main interdependent processes, operating synergistically to remove pollutants: electrochemistry, coagulation and hydrodynamics.

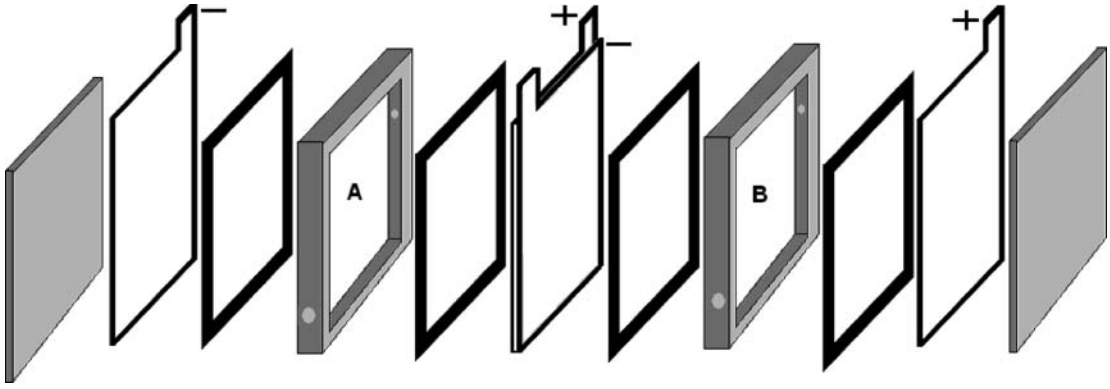

Fig. 3. Schematic view of Bipolar Electrocoagulation flow cell configuration.

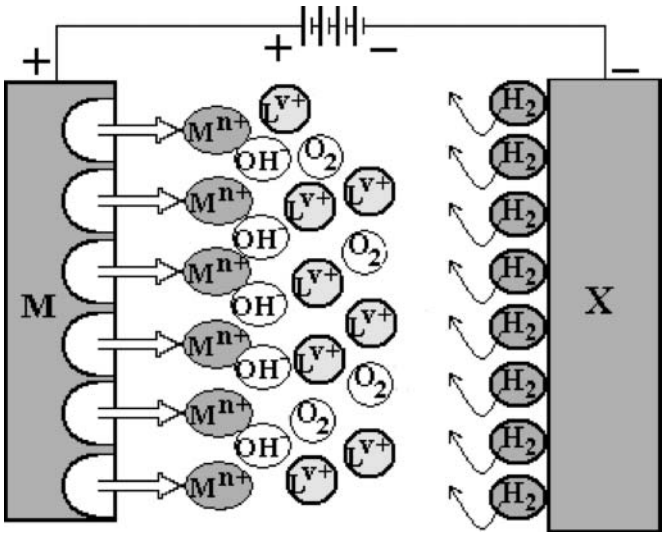

Fig. 4. A conceptual diagram of the electrocoagulation mechanism.

In an EC process, the coagulating ions are produced in situ involving three successive stages: (i) formation of coagulants by electrolytic oxidation of the "sacrificial electrode", such as aluminum, (ii) destabilization of the contaminants, particulate suspension and breaking of emulsions, (iii) aggregation of the destabilized phases to form flocs. Al gets dissolved from the anode generating corresponding metal ions, which almost immediately hydrolyze to polymeric aluminum oxyhydroxides. These polymeric oxyhydroxides are excellent coagulating agents. Figure 4 shows a conceptual diagram of the electro coagulation mechanism. The anodic reaction involves the dissolution of metal, and the cathodic reaction involves the formation of hydrogen gas and hydroxide ions.

At the Anode:

$$Al(s) \rightarrow Al^{3+} + 3e^{-} \tag{3}$$

At the Cathode

$$3H_2O + 3^{e-} \rightarrow (3/2)H_2(g) + 3OH^{-} \tag{4}$$

In bulk solution:

$$Al^{3+}(aq) + 3H_2O \rightarrow Al(OH)^{3+}(s) + 3H^{+} \tag{5}$$

Other reactions may be also encountered in anodic compartment is as follows:

$$2OH^{-} \rightarrow {}^{1/2}O_2 + H_2O + 2e^{-} \tag{6}$$

$$2Cl^{-} \rightarrow Cl_2 + 2e^{-} \tag{7}$$

$$Cl^{-} + 2OH^{-} \rightarrow OCl^{-} + H_2O + 2e^{-} \tag{8}$$

The main reaction encountered in the cathodic compartment is as follows:

$$2H_2O + 2e^{-} \rightarrow H_2 + 2OH^{-} \tag{9}$$

Al^{3+} and OH^{-} ions generated via electrode reactions (1) and (2) react to form various monomeric species, such as $Al(OH)^{2+}$, $Al(OH)_2^{+}$, $Al_2(OH)_2^{4+}$, $Al(OH)_4^{-}$; and polymeric species, such as $Al_6(OH)_{15}^{3+}$, $Al_7(OH)_{17}^{4+}$, $Al_8(OH)_{20}^{4+}$, $Al_{13}O_4(OH)_{24}^{7+}$, $Al_{13}(OH)_{34}^{5+}$; which transform finally into $Al(OH)^{3+}(s)$, which are partly soluble in the water under definite pH values. This step results in the colloidal particles formation and its structures is as given here:

$$\overbrace{\underbrace{\{[Al(OH)_3]_m}_{\text{Nucleus}}/\underbrace{nAl^{3+}(3n-x)\,Anion^{-}\}^{+}}_{\text{Adsorption Layer}}}^{\text{Granule}} + \underbrace{x\,Anion^{-}}_{\text{Diffusion Layer}} \tag{10}$$

$Al(OH)^{3+}(s)$ form the nucleus of a colloidal particle. Around the nucleus, the adsorption layer of cations and anions is being organized. The nucleus and adsorption layer form a granule of the colloidal particle, which has a small positive charge. To compensate the charge, a diffusion layer is being formed around the granule, which makes the particle a neutral one. Aluminum hydroxides that are formed in the process of the EC possess very high ability for absorption. Coagulated particles attract and absorb different ions and micro-colloidal particles from the wastewater. The flocks formed in the water are transported to the surface by the bubbles of gases (H_2 and O_2, etc.) produced in the process of electrolysis. As the solution contains Cl^{-} ions, Cl_2 will be liberated on the anode.

According to following complex precipitation kinetics, $Al(OH)^{3+}(s)$ adsorb the organic particles from the wastewater by electrocoagulation process and reduce COD in wastewater. In surface complexation mode, the pollutant acts as a ligand (L) to chemically bind hydrous aluminum:

$$L - H(aq)(OH)OAl(s) \rightarrow L \cdot OAl(s) + H_2O \tag{11}$$

The prehydrolysis of Al^{3+} cations also leads to the formation of reactive clusters for treatment. The contribution of separation by agglomeration of the particles by precipitation mechanism is predominant when pH is low, while adsorption plays a major role of separation mechanism in the case of operation at neutral to higher pH levels. The strong oxidizing agents produced in situ can take part in destructing the organic matter present in the waste by oxidizing them:

$$2Cl^{-} \rightarrow Cl_2 + 2e^{-} \tag{7}$$

$$Cl_2 + H_2O \rightarrow H^{+} + Cl^{-} + HOCl \tag{12}$$

$$HOCl \leftrightarrow H^{+} + OCl^{-} \tag{13}$$

$$HQ + OCl^{-} \rightarrow CO_2 + H_2O + Cl^{-} \tag{14}$$

In cathode the following reactions takes place

$$2H_3O^{+} + 2e^{-} \rightarrow H_2 + 2H_2O \qquad pH > 7 \tag{15}$$

$$2H_2O + 2e^{-} \rightarrow H_2 + 2OH^{-} \qquad pH < 7 \tag{16}$$

Table 2. The actual design of experiments and response for the percentage of COD removal and specific energy consumption in monopolar configuration.

S. No	Factor A: HQ conc. ($mg\ L^{-1}$)	Factor B: Supporting electrolyte conc. ($g\ L^{-1}$)	Factor C: Flow rate ($mL\ min^{-1}$)	Factor D: Current density ($A\ dm^{-2}$)	COD removal X (%)	Specific energy consumption E ($kW\ h\ (kg\ COD)^{-1}$)
1	1000	4	35	0.6	69.23	2.75
2	625	2.5	25	0.2	66.67	0.8
3	625	1	35	1	71.43	20.5
4	25.	2.5	25	0.6	75	10.88
5	625	1	25	0.6	61.9	9.69
6	625	2.5	35	0.6	61.9	5.54
7	250	2.5	35	0.2	50	0.8
8	250	2.5	45	0.6	75	10.88
9	1000	1	35	0.6	69.23	7.25
10	1000	2.5	35	0.2	61.54	0.75
11	625	2.5	45	1	71.43	10.75
12	625	4	25	0.6	76.19	3.23
13	625	2.5	35	0.6	61.9	5.54
14	250	2.5	35	1	62.5	33
15	625	2.5	45	0.2	66.67	0.86
16	1000	2.5	45	0.6	61.54	4.07
17	625	2.5	35	0.6	61.9	5.54
18	1000	2.5	35	1	73.08	8.49
19	625	2.5	35	0.6	61.9	5.54
20	625	1	45	0.6	52.38	11.05
21	625	4	35	0.2	61.9	0.64
22	1000	2.5	25	0.6	76.92	3.26
23	625	1	35	0.2	47.62	1.8
24	625	2.5	35	0.6	61.9	5.54
25	625	4	45	0.6	66.67	3.54
26	625	2.5	25	1	76.19	9.84
27	250	1	35	0.6	50	32.63
28	625	4	35	1	80.95	6.39
29	250	4	35	0.6	75	7.88

The specific energy consumption (E) for flow reactors is obtained using the following expressions.

$$\text{Specific Energy Consumption (E)} = \frac{VI}{3600 \times 10^3} \times \frac{1}{\Delta C \times Q \times 10^{-6}} \quad (17)$$

Where ΔCis the difference in COD in mg L^{-1}, due to the treatment by passing I current for t seconds. V is the voltage (V), Q represents the volumetric flow rate in L s^{-1}.

Experimental design and optimization

HQ concentration, supporting electrolyte concentration, flow rate, current density were chosen as independent variables and the % of COD removal, energy consumption as dependent output response variables. Independent variables, experimental range and levels for COD removal are given in Table 1. Experimental plan showing the actual value of the variables together with COD removal efficiency and energy consumption for monopolar and bipolar configuration are given in Table 2 and 3. The behavior of the system was explained by the following quadratic equation

$$\eta = \beta_o + \sum_{i=1}^{k} \beta_i x_i + \sum_{i=1}^{k} \beta_{ii} x_i^2 + \sum_{i=1}^{k-1} \sum_{j=2}^{k} \beta_{ij} x_i x_j + \varepsilon \quad (18)$$

Where η is the response, xi and xj are coded independent variables (i = 1 to k), β_0 is the constant coefficient, βi, βii and βij (i and j = 1 to k) are the regression coefficients for the intercept, linear, quadratic and the interaction terms, respectively, k is the number of independent parameters and ε is the statistical error. The results of the experimental design were studied and interpreted by Design Expert Software-7.1.2, Stat-Ease, Inc., Minneapolis, USA, (trial version) to estimate the response of the dependent variable.

Table 3. The actual design of experiments and response for the percentage COD removal and specific energy consumption in bipolar configuration.

S. No	*Factor A: HQ conc.* ($mg\ L^{-1}$)	*Factor B: Supporting electrolyte conc.* ($g\ L^{-1}$)	*Factor C: Flow rate* ($mL\ min^{-1}$)	*Factor D: Current density* ($A\ dm^{-2}$)	*COD removal X* (%)	*Specific energy consumption E* ($kW\,h\ (kg\ COD)^{-1}$)
1	1000	4	35	0.6	84.62	4.91
2	625	2.5	25	0.2	71.43	1.6
3	625	1	35	1	85.71	40.63
4	250	2.5	25	0.6	87.5	20.89
5	625	1	25	0.6	76.19	13.78
6	625	2.5	35	0.6	76.19	9
7	250	2.5	35	0.2	62.5	4.95
8	250	2.5	45	0.6	75	23.25
9	1000	1	35	0.6	76.92	14.29
10	1000	2.5	35	0.2	73.08	1.22
11	625	2.5	45	1	80.95	20.51
12	625	4	25	0.6	80.95	6.22
13	625	2.5	35	0.6	76.19	9
14	250	2.5	35	1	87.5	51.96
15	625	2.5	45	0.2	66.67	1.71
16	1000	2.5	45	0.6	69.23	8.25
17	625	2.5	35	0.6	76.19	9
18	1000	2.5	35	1	84.62	15.85
19	625	2.5	35	0.6	76.19	9
20	625	1	45	0.6	61.9	21.63
21	625	4	35	0.2	76.19	1.31
22	1000	2.5	25	0.6	73.08	7.82
23	625	1	35	0.2	66.67	2.95
24	625	2.5	35	0.6	76.19	9
25	625	4	45	0.6	71.43	7.05
26	625	2.5	25	1	90.48	18.36
27	250	1	35	0.6	75	49.5
28	625	4	35	1	90.48	13.42
29	250	4	35	0.6	87.5	20.25

Results and discussion

Experiments according to the design in Tables 2 and 3 were carried out and relevant results are shown in Tables 2 and 3, which lists the percentage of COD removal (X) and specific energy consumption (E). The relationship between four controllable factors (such as HQ concentration, supporting electrolyte concentration, flow rate and current density) and % of COD removal and specific energy consumption for the electrocoagulation process has been studied.

The response surface methodology has been successfully applied for optimizing conditions for hydroquinone removal from wastewater. Range and level of input factors chosen in this study are presented in Table 1.

Tables 2 and 3 show the data resulting from the experiment of the effect of four variables such as HQ concentration (A), supporting electrolyte concentration (B), flow rate (C) and current density (D) on the percentage of COD removal (X) and specific energy consumption (E). The experimental results were analyzed through RSM to obtain an empirical model for the best response. The estimated response seems to have a functional relationship only in a local region or near the central point of the model. The quadratic model was used to explain the mathematical relationship between the independent variables and dependent responses. The mathematical expressions of relationship to the % of COD removal and specific energy consumption with variables like A, B, C and D are shown below as in terms of coded factors for monopolar and bipolar configuration, respectively.

Monopolar :

$$\begin{aligned}&\%\ \text{of COD Removal, X}\\&= 76.19 - 1.12\,\mathrm{A} + 4.06\,\mathrm{B} - 4.54\,\mathrm{C}\\&+ 8.60\,\mathrm{D} - 1.20\mathrm{AB} + 2.16\mathrm{AC} - 3.36\mathrm{AD}\\&+ 1.19\mathrm{BC} - 1.18\mathrm{BD}1.19\mathrm{CD}\\&+ 1.66\mathrm{A}^2 + 1.28\,\mathrm{B}^2 - 2.31\,\mathrm{C}^2 + 1.62\,\mathrm{D}^2 \qquad (19)\end{aligned}$$

Table 4. ANOVA results for the percentage of COD removal in monopolar configuration.

Source	*Degrees of freedom*	*Sum of squares*	*Mean square*	*F-value*	*P*
Model	14	1682.64	120.19	3.77	0.0091
Residual	14	446.09	31.86		significant
Lack of fit	10	446.09	44.61		
Pure error	4	0.000	0.000		
total	28	2128.73			

S.D: 5.64; R^2: 0.7904; adj: R^2 0.5809.

Table 6. ANOVA results for the percentage of COD removal in bipolar configuration.

Source	*Degree of freedom*	*Sum of square*	*Mean square*	*F-value*	*P*
Model	14	1528.76	109.2	7.43	0.0003
Residual	14	205.66	14.69		significant
Lack of fit	10	205.66	20.57		
Pure error	4	0.000	0.000		
total	28	1734.42			

S.D: 3.83; R^2: 0.8814; adj: R^2 0.7628.

and

$$\text{Specific energy Consumption, E} = +9.00 - 6.16\text{A} - 3.75\text{B} + 1.14\,\text{C} + 12.25\,\text{D} - 6.17\text{AB} - 0.48\text{AC} - 8.10\text{AD} - 1.75\text{BC} - 6.39\text{BD} + 0.51\text{CD} + 4.17\text{A}^2 + 0.76\,\text{B}^2 + 0.72\text{C}^2 + 3.65\,\text{D}^2 \quad (20)$$

$$\text{Bipolar : \% of COD Removal, X} = 76.19 - 1.12\,\text{A} + 4.06\,\text{B} - 4.54\,\text{C} + 8.60\,\text{D} - 1.20\text{AB} + 2.16\text{AC} - 3.37\text{AD} + 1.19\text{BC} - 1.19\text{BD} - 1.19\text{CD} + 1.66\text{A}^2 + 1.28\,\text{B}^2 - 2.31\,\text{C}^2 + 1.62\,\text{D}^2 \quad (21)$$

and

$$\text{Specific energy Consumption, E} = +9.0 - 9.87\,\text{A} - 7.47\,\text{B} + 1.15\,\text{C} + 12.25\,\text{D} + 4.97\text{AB} - 0.48\,\text{AC} - 8.10\,\text{AD} - 1.76\,\text{BC} - 6.39\,\text{BD} + 0.51\text{CD} + 7.88\,\text{A}^2 + 4.48\,\text{B}^2 - 1.13\,\text{C}^2 + 1.80\,\text{D}^2 \quad (22)$$

The results of analysis of variance for monopolar configuration (ANOVA) are shown in Table 4, which indicates that the predictability of the model for % of COD Removal, X, is at 95% confidence interval. The predicted responses fit well with those of the experimentally obtained responses. A coefficient of determination (R^2) value of 0.7904 showed that the equation is highly reliable. Further the computed F-value (3.77) is greater than that of the tabular value $F_{0.01(14,14)}$ value (3.70), suggesting that the treatment is significant. A 'P'-value less than 0.01 indicate that the model is statistically significant. Similarly Table 5 indicates that the predictability of the model for specific energy consumption, E is at 95% confidence interval. The predicted responses fit well with those of the experimentally obtained responses. A coefficient of determination (R^2) value of 0.7686 showed that the equation is highly reliable. Further, the computed F-value (3.32) is greater than that of the tabular value $F_{0.01(14,14)}$ value (3.70) suggesting that the treatment is significant. A 'P'-value less than 0.01 indicate that the model is statistically significant.

The results of analysis of variance for bipolar configuration (ANOVA) are shown in Table 6, which indicates that the predictability of the model for % of COD Removal, X, is at 95% confidence interval. The predicted responses fit well with those of the experimentally obtained responses. A coefficient of determination (R^2) value of 0.8814 showed that the equation is highly reliable better than mono polar configuration. Further the computed F-value (7.43) is greater than that of the tabular value $F_{0.01(14,14)}$ value (3.70) suggesting that the treatment is significant. A 'P'-value less than 0.01 indicate that the model is statistically significant. Similarly Table 7 indicates that the predictability of the model Specific energy Consumption, E is at 95% confidence interval. The predicted responses fit well with those of the experimentally obtained responses. A coefficient of determination (R^2) value of 0.8635 showed that the equation is highly reliable. Further the computed F-value (6.32)

Table 5. ANOVA results for the specific energy consumption in monopolar configuration.

Source	*Degree of freedom*	*Sum of square*	*Mean square*	*F-value*	*P*
Model	14	945.64	6.55	3.32	0.016
Residual	14	284.77	20.34		significant
Lack of fit	10	284.77	28.48		
Pure error	4	0.000	0.000		
total	28	1230.4			

S.D: 4.51; R^2: 0.7686; adj: R^2 0.5371.

Table 7. ANOVA results for the specific energy consumption in bipolar configuration.

Source	*Degrees of freedom*	*Sum of squares*	*Mean square*	*F-value*	*P*
Model	14	3203.31	228.81	6.32	0.0007
Residual	14	506.54	36.18		significant
Lack of fit	10	506.54	50.65		
Pure error	4	0.000	0.000		
total	28	3709.85			

S.D: 6.02; R^2: 0.8635; adj: R^2 0.7269.

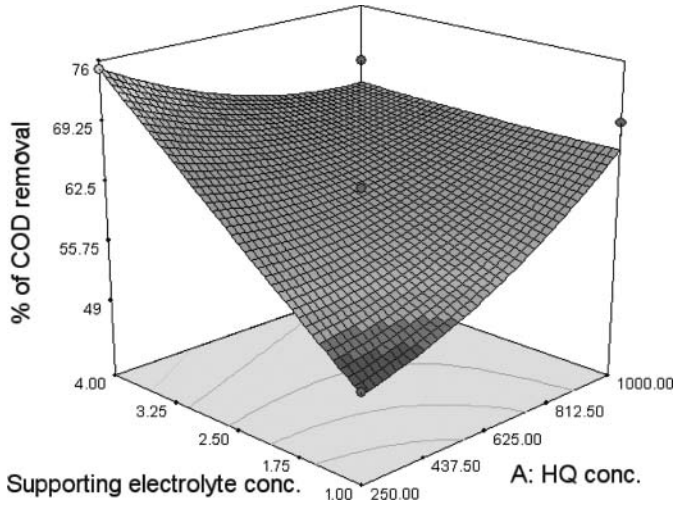

Fig. 5. Response surface plot showing the effect of concentration of HQ and SE on % of COD removal (Conditions: Q 35 mL · min^{-1}; CD 0.6 A · dm^{-2}; configuration: monopolar).

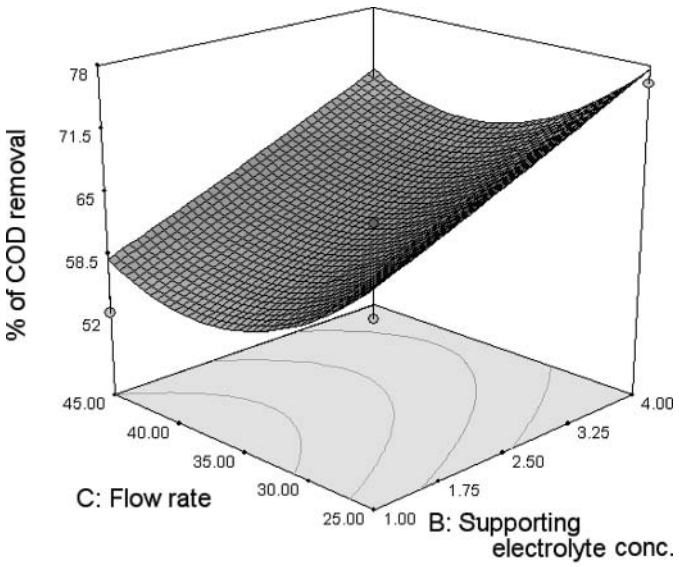

Fig. 7. Response surface plot showing the effect of Q and concentration of SE on % of COD removal (Conditions: Conc. of HQ 625 mg · L^{-1}; CD 0.6 A · dm^{-2}; configuration: monopolar).

is greater than that of the tabular value $F_{0.01(14,14)}$ value (3.70) suggesting that the treatment is significant. A '*P*'= value less than 0.01 indicates that the model is statistically significant better than mono polar configuration.

Using RSM the combined effect of 4 variables can be predicted which is difficult to observe in conventional methods. The effects of variables on HQ removal in monopolar configuration are shown through Figures 5–9 and the effects of variables on HQ removal in bipolar configuration are shown through Figures 10–14.

Figure 5 shows the 3D response surface plot of interaction between varying concentration of hydroquinone and supporting electrolyte concentration on percentage of COD removal at 35 mL · min^{-1} flow rate and 0.6 A · dm^{-2} current density. It can be ascertained from the surface plot that the COD removal increases with increasing supporting electrolyte concentration and decreasing hydroquinone concentration. This is because an increase in supporting electrolyte concentration increases the mobility of ions in the solution, and in turn, increases the COD removal. On the other hand, the ratio of hydroquinone concentration

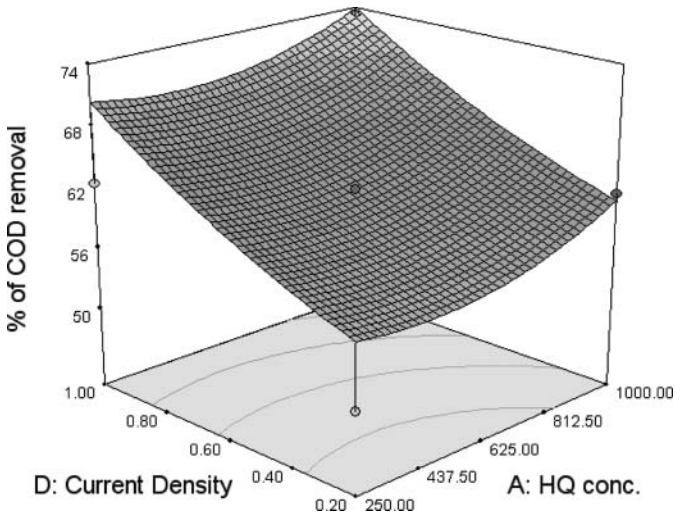

Fig. 6. Response surface plot showing the effect of concentration of HQ and CD on % of COD removal (Conditions: Q 35 mL · min^{-1}; conc. of SE 2.5 g · L^{-1}; configuration: monopolar).

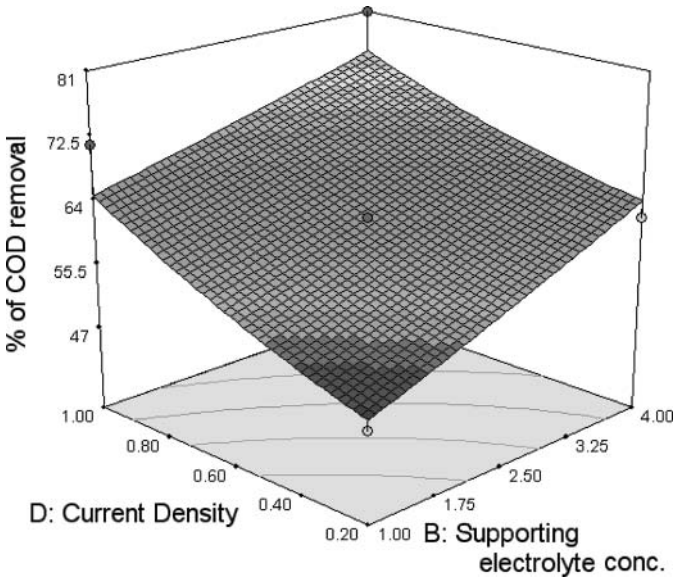

Fig. 8. Response surface plot showing the effect of CD and concentration of SE on % of COD removal (Conditions: Conc. of HQ 625 mg·L^{-1}; Q 35 mL·min^{-1}; configuration: monopolar).

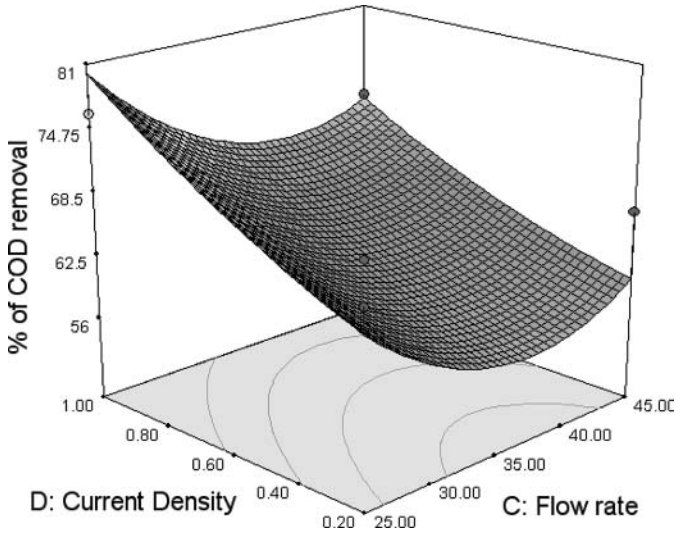

Fig. 9. Response surface plot showing the effect of CD and Q on % of COD removal (Conditions: Conc. of HQ 625 mg·L^{-1}; Conc. of SE 2.5 g·L^{-1}; configuration: monopolar).

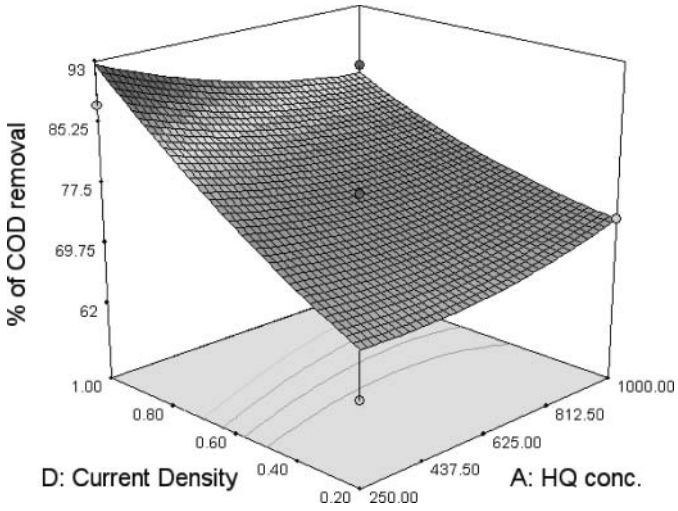

Fig. 11. Response surface plot showing the effect of concentration of HQ and CD on % of COD removal (Conditions: Q 35 mL · min^{-1}; conc. of SE 2.5 g · L^{-1}; configuration: bipolar).

to OCl^- radial concentration increased with initial hydroquinone concentration, and in turn, decreases with COD removal. Maximum percentage of COD removal was observed at low hydroquinone (250 mg L^{-1}) and high supporting electrolyte concentration (4 g L^{-1}). The percentage of COD removal was decreased with increase in hydroquinone concentration, even in the presence of high supporting electrolyte concentration (4 g · L^{-1}). At high hydroquinone concentration the efficiency of supporting electrolyte reduced but did not completely diminish. The surface plot also shows the best COD removal (75%) obtained at 250 mg · L^{-1} hydroquinone and 4 g · L^{-1} of supporting electrolyte.

Figure 6 represents the effect of hydroquinone concentration and current density at fixed supporting electrolyte concentration and flow rate. Maximum COD removal was 72% for 250 mg L^{-1} hydroquinone at 1 A · dm^{-2} current density when keeping the flow rate and electrolyte concentration at 35 mL · min^{-1} and 2.5 g · L^{-1} , respectively. COD removal increased with increase in current density, because the rate of generation of Al^{3+} ions increased with current density, which eventually increased the COD reduction.

Figure 7 represents the effect of supporting electrolyte concentration and flow rate at fixed concentration of hydroquinone and current density. Maximum COD removal

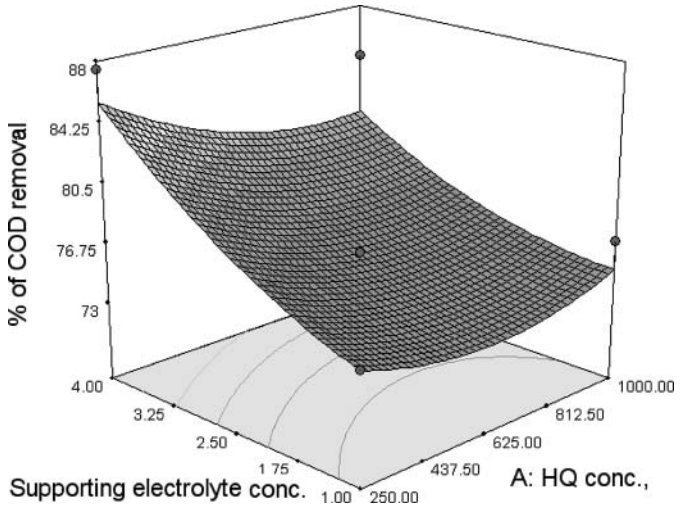

Fig. 10. Response surface plot showing the effect of concentration of HQ and SE on % of COD removal (Conditions: Q 35 mL·min^{-1}; CD 0.6 A·dm^{-2}; configuration: bipolar).

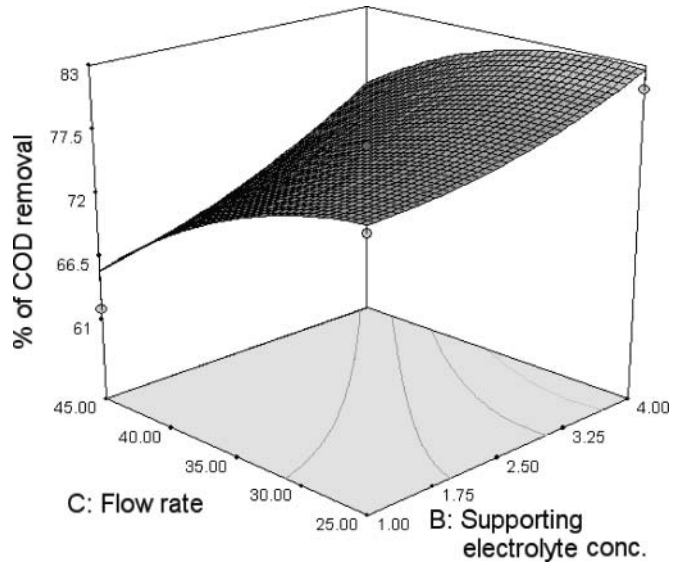

Fig. 12. Response surface plot showing the effect of Q and concentration of SE on % of COD removal (Conditions: Conc. of HQ 625 mg · L^{-1}; CD 0.6 A · dm^{-2}; configuration: bipolar).

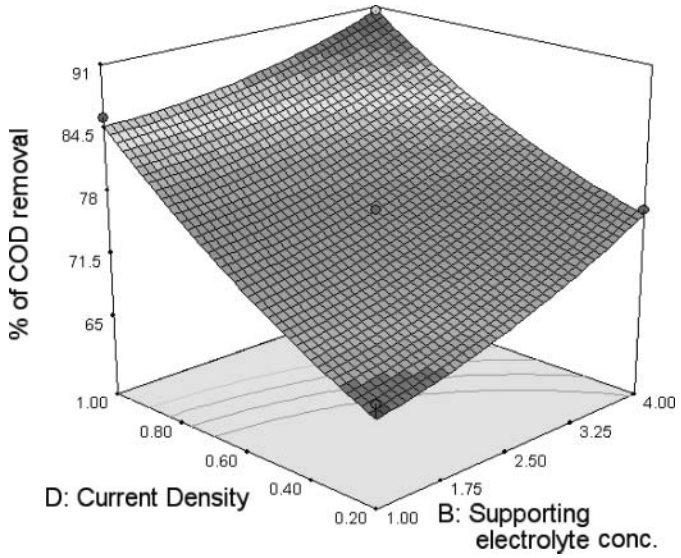

Fig. 13. Response surface plot showing the effect of CD and concentration of SE on % of COD removal (Conditions: Conc. of HQ 625 mg · L^{-1}; Q 35 mL · min^{-1}; configuration: bipolar).

was 77% for 625 mg · L^{-1} hydroquinone concentration at high supporting electrolyte concentration (4 g · L^{-1}) and low flow rate (25 mL · min^{-1}). COD removal increased with increasing supporting electrolyte concentration. On the other hand, COD removal slightly decreased when increasing the flow rate of wastewater. Hence, retention time decreased when increasing the flow rate.

Figure 8 represents the effect of varying supporting electrolyte concentration and different current density at fixed concentration of hydroquinone and flow rate. It can be ascertained from the surface plot that the COD removal

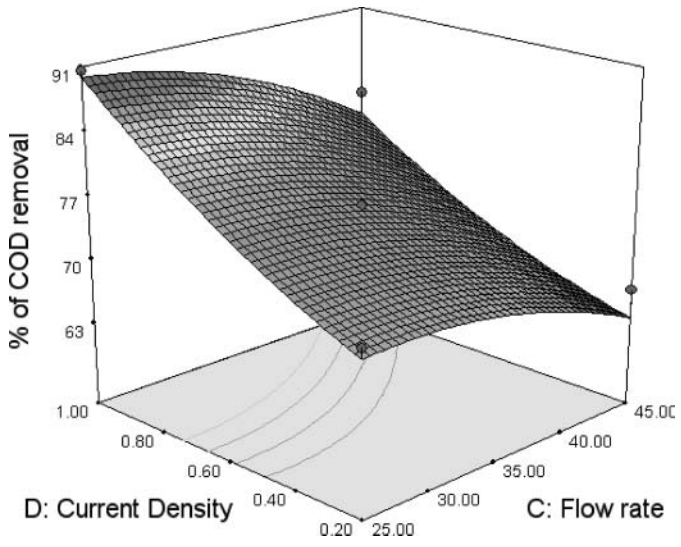

Fig. 14. Response surface plot showing the effect of CD and Q on % of COD removal (Conditions: Conc. of HQ 625 mg · L^{-1}; Conc. of SE 2.5 g · L^{-1}; configuration: bipolar).

increases with increasing supporting electrolyte concentration and increases with current density. So current density and supporting electrolyte concentration is very important for COD removal in flow electro coagulation process. 74 % of COD was removed at high supporting electrolyte concentration (4 g · L^{-1}) and high current density (1 A dm^{-2}) for 625 mg L^{-1} hydroquinone at 35 mL · min^{-1} flow rate.

Figure 9 represents the effect of varying flow rate and different current density. It can be ascertained from the surface plot that the COD removal increased with increase in current density, because the rate of generation of Al^{3+} ions increased with current density, which eventually increased the COD reduction. But flow rate is slightly effect the efficiency of COD removal compared to current density. Then 80% of COD was removed at high current density (1 A · dm^{-2}) and low flow rate (25 mL · min^{-1}) for 625 mg · L^{-1} of HQ concentration in 2.5 g · L^{-1} of supporting electrolyte concentration.

Figure 10 shows the 3D response surface plot of interaction between varying concentration of hydroquinone and supporting electrolyte concentration on percentage of COD removal at 35 mL · min^{-1} flow rate and 0.6 A · dm^{-2} current density. It can be ascertained from the surface plot that the COD removal increases with increasing supporting electrolyte concentration and decreases with increasing hydroquinone concentration. This is because an increase in supporting electrolyte concentration increases the mobility of ions and in turn, increases the COD removal. On the other hand, the ratio of hydroquinone concentration to OCl^- radial concentration increased with initial hydroquinone concentration, and in turn, decreases with COD removal. Maximum % of COD removal was observed at low hydroquinone (250 mg L^{-1}) and high supporting electrolyte concentration (4 g · L^{-1}). The percentage of COD removal was decreased with increase in hydroquinone concentration even in the presence of high supporting electrolyte concentration (4 g L^{-1}). At high hydroquinone concentration the efficiency of supporting electrolyte reduced but did not completely diminish. The surface plot also shows the best COD removal (86%) obtained at 250 mg · L^{-1} hydroquinone and 4 g L^{-1} of supporting electrolyte.

Figure 11 represents the effect of varying hydroquinone concentration and current density at fixed supporting electrolyte concentration and flow rate. Maximum COD removal was 90.4% for 250 mg · L^{-1} hydroquinone at 1 A · dm^{-2} current density when keeping the flow rate and electrolyte concentration at 35 mL · min^{-1} and 2.5 g · L^{-1}, respectively. COD removal increased with increase in current density, because the rate of generation of Al^{3+} ions increased with current density, which eventually increased the COD reduction.

Figure 12 represents the effect of varying supporting electrolyte concentration and different flow rate at fixed concentration of hydroquinone and current density. Maximum COD removal was 82% for 625 mg L^{-1} hydroquinone concentration at high supporting electrolyte concentration

(4 g · L^{-1}) and low flow rate (25 mL · min^{-1}). COD removal linearly increased with increasing supporting electrolyte concentration. On the other hand, COD removal slightly decreased when increasing the flow rate of wastewater. Hence, retention time decreased when increasing the flow rate.

Figure 13 represents the effect of varying supporting electrolyte concentration and different current density at fixed concentration of hydroquinone and flow rate. It can be ascertained from the surface plot that the COD removal increases with increasing supporting electrolyte concentration and increases with current density. So current density and supporting electrolyte concentration is very important for COD removal in flow electro coagulation process. Then, 90.4% of COD was removed at high supporting electrolyte concentration (4 g · L^{-1}) and high current density (1 A · dm^{-2}) for 625 mg L^{-1} hydroquinone at 35 mL · min^{-1} flow rate.

Figure 14 represents the effect of varying different flow rate and different current density. It can be ascertained from the surface plot that the COD removal increased with increase in current density, because the rate of generation of Al^{3+} ions increased with current density, which eventually increased the COD reduction. But flow rate is slightly effect the efficiency of COD removal while compare with current density. Then, 89% of COD was removed at high current density (1 A · dm^{-2}) and low flow rate (25 mL · min^{-1}) for 625 mg · L^{-1} concentration at 2.5 g · L^{-1} of supporting electrolyte concentration.

Conclusion

Experiments were carried out on removal of hydroquinone in flow eletrolyzer (electro coagulation technique) covering wide range of operating conditions in monopolar and bipolar configurations. The influence of hydroquinone concentration, supporting electrolyte concentration, flow rate and current density on the rate of degradation was critically examined. It was observed from this investigation that the percentage of COD reduction is significantly influenced by the hydroquinone concentration, supporting electrolyte concentration, flow rate and current density. Current density and supporting electrolyte concentration are the important factors for degradation of hydroquinone.

The experimental data were analyzed using response surface methodology and the individual and combined parameter effects on COD reduction were analyzed. Three levels and four factors Box-Behnken experimental design was applied. Regression equation were developed for COD removal and energy consumption using sets of experimental data and solved using the Design Expert software. It was observed that model predictions of COD removal and energy consumption are in good agreement with experimental observations. Further, the parameters were optimized for effective degradation of hydroquinone in flow electrolyzer using response surface method. The optimized values for 80.95% of COD removal through electro-coagulation are: supporting electrolyte concentration 2.67 g · L^{-1}, flow rate 27 mL · min^{-1}, 0.7 Adm^{-2} and energy consumption of 2.36 kWh per kg of COD for the 1000 mg · L^{-1} of hydroquinone concentration in monopolar configuration and 87.13 % of COD removal through electro-coagulation are: supporting electrolyte concentration 4 g · L^{-1}, flow rate 29.15 mL · min^{-1}, 1 A · dm^{-2} and energy consumption of 8.495 kWh per kg of COD for the 1000 mg · L^{-1} of hydroquinone concentration in bipolar configuration.

Acknowledgment

Authors greatly acknowledge the Director, Central Electrochemical Research Institute, Karaikudi, India for his constant encouragement.

References

[1] Hydroquinone, Environmental Health Criteria 157, International Programme on Chemical Safety (1994), www.inchem.org/documents/**ehc/ehc/ehc157**.htm and www.inchem.org/documents/hsg/hsg/hsg101.htm

[2] Chitra, S.; Sekaran, G.; Padmavathi, S.; Chandrakasan, G. Removal of phenolic compounds from wastewater using mutant strain of Pseudomonas pictorum. J. Gen. Appl. Microbiol. **1995**, *41*(33), 229–237.

[3] Perez, R.R.; Benito, G.G.; Miranda, M.P. Chlorophenol degradation by Phanerochaete chrysosporium. Bioresource Tech. **1997**, *60*(3), 207–213.

[4] Slokar, Y.M.; Le Marechal, A.M. Methods of decoloration of textile wastewaters, Dyes and Pigments **1998**, *37*(4), 335–356.

[5] Wang, Y. Solar photo catalytic degradation of eight commercial dyes in TiO_2 suspension. Water Res. **2000**, *34*(3), 990–994.

[6] Pearce, C.I.; Lloyd, J.R.; Guthrie, J.T. The removal of color from textile wastewater using whole bacterial cells: a review. Dyes Pigments **2003**, *58*(3), 179–196.

[7] Tanaka, K.; Padermpole, K.; Hisanaga, T. Photocatalytic degradation of commercial azo dyes. Water Res. **2000**, *34*(1), 327–333.

[8] Suksaroj, C.; Heran, M.; Allegre, C.; Persin, F. Treatment of textile plant effluent by nanofiltration and/or reverse osmosis for water reuse. Desalination **2005**, *178*(1–3), 333–341.

[9] Baban, A.; Yedilar, A.; Lienert, D.; Kemerder, N.; Kettrup, A. Ozonation of high strength segregated effluents from a woollen textile dyeing and finishing plant. Dyes and Pigments **2003**, *58*(2), 93–98.

[10] Adhoum, N.; Monser, L.; Bellakhal, N.; Belgaied, J.E. Treatment of electroplating wastewater containing Cu^{2+}, Zn^{2+} and Cr^{6+} by electrocoagulation. J. Hazard. Mater. **2004**, *112*(3), 207–213.

[11] Hunsom, M.; Pruksathorn, K.; Damronglerd, S.; Vergnes, H.; Duverneuil, P. Electrochemical treatment of heavy metals (Cu^{2+}, Cr^{6+}, Ni^{2+}) from industrial effluent and modeling of copper reduction, Water Res. **2005**, *39*(4), 610–616.

[12] Ratna Kumar, P.; Chaudhari, S.; Khilar, K.C.; Mahajan, S.P. Removal of arsenic from water by electro coagulation. Chemosphere **2004**, *55*(9), 1245–1252.

[13] Gao, P.; Chen, X.; Shen, F.; Chen, G. Removal of chromium (VI) from wastewater by combined electro coagulation–electro flotation without a filter. Sep. Purif. Technol. **2005**, *43*(2), 117–123.

[14] Matteson, M.J.; Dobson, R.L.; Glenn, R.W.; Kukunoor, N.S.; Waits, W.H.; Clayfield, E.J. Electro coagulation and separation of aqueous suspensions of ultra fine particles. Coll. Surf. A **1995**, *104*(1), 101–109.
[15] Holt, P.K.; Barton, G.W.; Mitchell, C.A. Deciphering the science behind electro coagulation to remove suspended clay particles from water. Water Sci. Technol. **2004**, *50*(12), 177–184.
[16] Xu, X.; Zhu, X.; Treatment of refectory oily wastewater by electro coagulation process. Chemosphere **2004**, *56*(10), 889–894.
[17] Murugananthan, M.; Bhaskar Raju, G.; Prabhakar, S. Separation of pollutants from tannery effluents by electro flotation. Sep. Purif. Technol. **2004**, *40*(1), 69–75.
[18] Jiang, J.Q.; Graham, N.; Andre, C.; Kelsall, G.H.; Brandon, N. Laboratory study of electro coagulation-flotation for water treatment. Water Res. **2002**, *36*(16), 4064–4074.
[19] Mameri, N.; Yeddou, A.R.; Lounici, H.; Belhocine, D.; Grib, H.; Bariou, B. Defluoridation of septentrional Sahara water of North Africa by electro coagulation process using bipolar aluminium electrodes. Water Res. **1998**, *32*(5), 1604–1612.
[20] Yousuf, M.; Mollah, A.; Schennach, R.; Parga, J.R.; Cocke, D.L. Electro coagulation (EC)-science and applications. J. Hazard. Mater. **2001**, *84*(1), 29–41.
[21] Lin, S.H.; Shyu, C.T.; Sun, M.C. Saline wastewater treatment by electrochemical method. Water Res. **1998**, *32*(4), 1059–1066.
[22] Lin, S.H.; Peng, C.F. Continuous treatment of textile wastewater by combined coagulation electrochemical oxidation and activated sludge. Water Res. **1996**, *30*(3), 587–592.
[23] Tsai, C.T.; Lin, S.T.; Shue, Y.C.; Su, P.L. Electrolysis of soluble organic matter in leachate from landfills. Water Res. **1997**, *31*(12), 3073–3081.
[24] Szewzyk, U.; Schink, B. Methanogenic Degradation of hydroquinone in an anaerobic fixed-bed reactor. Appl. Biotechnol. Microbiol. **1989**, *32*(3), 346–349.
[25] Kelly, C.J.; Lajoie, C.A.; Layton, A.C.; Sayler, G.S. Bioluminescent Reporter Bacterium for Toxicity Monitoring in Biological Wastewater Treatment Systems. Water Environ. Res. **1999**, *71*(1), 31–35
[26] Clesceri, L.S.; Greenberg, A.E.; Eaton, A.D. *Standard Methods for the Examination of Water and Wastewater*. 1998, 20th edition. APHA, Washington, DC.
[27] Kwak, J.S. Application of Taguchi and response surface methodologies for geometric error in surface grinding process. Int. J. Machine Tools Manuf. **2005**, *45*(3) 327–334.
[28] Gunaraj, V.; Murugan, N. Application of response surface methodologies for predicting weld base quality in submerged arc welding of pipes. J. Mater Process Technol. **1999**, *88*(1–3), 266–275.
[29] Oliveira, F.S.; Sousa, E.T.; Andrade, J.B. A sensitive flow analysis system for the fluorimetric determination of low levels of formaldehyde in alcoholic beverages. Talanta, **2007**, *73*(3), 561–566.